Improving Resistance of Austenitic Stainless Steel to Irradiation Damage

P. Ahmedabadi[1], Vivekanand Kain[1], G. K. Dey[1] and I. Samajdar[2], S C Sharma[3], P Bhagwat[3], S Kailas[3]
[1]Materials Science Division, Bhabha Atomic Research Centre, India
[2]Indian Institute of Technology, Bombay, India, [3]Nuclear Physics Division, BARC, India
Email: id.parag@gmail.com

Abstract. It is believed that the addition of oversized solute atoms disturbs the process of recombination, agglomeration, and migration of point defects during irradiation process and thereby alters radiation damage, including radiation induced segregation. In this study, austenitic stainless steel (SS) 316 samples with different Ce content (0.00, 0.01, 0.04 and 0.09 wt% Ce) were irradiated using 4.8 MeV protons at 300^{o}C to the total fluence of 9.724×10^{17} p/cm^2. Irradiated samples were characterized using double-loop electrochemical potentiokinetic reactivation (DL-EPR) technique for the extent of RIS due to proton irradiation. It was found that the sample with 0.04 wt% Ce content showed the lowest EPR value, as measured by DL-EPR. It was also noticed that the slip lines were get preferentially attacked vis-à-vis grain boundaries. SS 316 Ce 0.09 wt% sample did not have any slip-lines and attack during the DL-EPR was confined to grain boundaries and few pit-like structures were noticed during AFM examinations.

1. Introduction

The addition of oversized solute atoms has been shown to disturb the process of recombination, agglomeration, and migration of point defects during irradiation process and thereby alters radiation damage [1-8], RIS and possibly IASCC. Several authors have studied the impact of oversized solute additions on radiation-induced changes in microstructure and microchemistry of austenitic stainless steels during irradiation. Kato et al.[5] investigated the influence of the addition of 0.35 at% of various oversized elements like Ti, Zr, Hf, V, Nb, and Ta on both RIS and void formation in 316L stainless steel, irradiated with electrons to 10.8 dpa at temperatures ranging from 400-500^{o}C. It was found that RIS behaviour of Cr and Ni strongly affected by the addition of oversized solutes. Hf and Zr addition were found to completely suppress RIS. Further studies on same alloys [7] irradiated with fast neutrons (up to 35 dpa) in the temperature range of 425-600^{o}C confirmed the beneficial effect of Hf and Zr addition. Shigenka et al.[10] performed 400 keV He^{+} irradiations on type 316L stainless steels with addition of 0.07, 0.21, or 0.41 wt% Zr up to 3.4 dpa. An almost complete suppression of Cr depletion at grain boundaries was noticed when the Zr content is higher than 0.21 wt%. Watanbe et al. [2] carried out electron irradiation studies on Fe-16Cr-17Ni pure ternary austenitic alloys doped with 0.1Nb and; beneficial effect of such addition on radiation-induced microstructure was observed at dose up to 2 dpa. Dumbill and Hanks [8] investigated the effect of Ti (0.18 wt %) and Nb (0.44 wt%) on RIS of type 304 SS irradiated with 46.5 Ni^{6+} ions up to 5 dpa. Ti and Nb both resulted in an important reduction of the extent of RIS at grain boundaries. Very little literature data dealing with the effect of oversized solute additions on IASCC are available. Kasahara et al. [3] have investigated the effect of 0.32 wt% Ti and Nb additions on IASCC of 316L stainless steels; neither addition of Ti nor Nb was found to improve IASCC resistance. However, Fournier et al [9] have observed the beneficial effect of addition of oversized solute elements Hf and Pt on resistance of type 316L SS toward IASCC. They also found that both Hf and Pt were beneficial in suppressing/retarding RIS on grain boundaries in type 316 SS. Samples of stainless steels were subjected to proton irradiation and subsequently to IGSCC in test in a simulated BWR environment. The beneficial effect of addition of oversized solute atoms was attributed to [1-9] reduction in point defect migration to the grain boundary and agglomeration into loops and voids by trapping migrating vacancies and subsequently increasing the recombination rate. The formation of Hf-vacancy [9] complexes and the subsequent enhancement of point defect

recombination is a plausible mechanism as it would result in a reduction in the partitioning of point defect flux to grain boundaries. Sakaguchi et al.[4] have considered that the oversized solute atoms interact with vacancies via the formation of an additive-vacancy complex. The influence of the linear size factor of the oversized solute atoms on RIS was model in [4]. The linear size fact, L_{sf} is defined as (in %),

$$L_{sf} = \left(\left(\frac{\Omega_{add}}{\Omega_{sol}}\right)^{1/3} - 1\right) \cdot 100 \qquad (1)$$

where sol, is the atomic volume of the solvent, add is the atomic volume of additive. Calculated linear size factor for various oversized solute atoms are given in Table 3.1 [9]. Model predictions were in good agreement with RIS measurements performed by Kato et al.[5] on model 316L SS doped with doped with different oversized elements. It can be seen from the Table 1 that Ce has the highest linear size factor among all elements depicted.

Table 1: Calculated linear size factor for various oversized solute elements

Element	Atomic number	Atomic volume (cm^3)	Linear Size Factor (%)
V	20	8.36	6.81
Pt	78	9.09	9.84
Ti	22	10.62	15.68
Nb	41	10.83	16.44
Ta	73	10.85	16.51
Zr	40	14.01	26.87
Hf	72	13.41	25.04
Ce	58	20.67	42.78

This would result in more strain energy with lattice and produce more strain energy. Thus, higher strain energy within the grains due Ce addition would be result in more effective hindrance toward the vacancy migration to defect sinks like grain boundaries. In earlier work, it has been reported that the effect of addition of cerium in steels, on their corrosion properties, is to form a thermodynamically stable surface film composed of cerium oxide [11]. This reduces the cathodic/anodic reactivity by blocking the reactive surface sites and improve resistance to pitting/crevice corrosion [11,12]. The addition of cerium is also reported to have improved the dry oxidation resistance [13, 14] of SS which was attributed to the larger atomic size of the rare earth element with respect to that iron. The vacancies in the alloy move to the stressed regions adjacent to the rare earth oxides at the metal/oxide interface where they serve as nucleation sites for chromium oxide and also affect the diffusion rate of chromium. SS 316 with Ce content have been shown to increase the resistance to sensitization [15] as well as IGSCC [16]. It was also shown that SS 316 with Ce content up to 0.01 wt% improves resistance to thermal sensitization as well as low temperature sensitization [15]. In view of this, type SS 316 with different Ce content of 0.0, 0.01, 0.04 and 0.09 wt% Ce were irradiated using proton to study the effect of over-sized solute addition on RIS. This paper describes, in detail, experiment setup used for irradiation and the effect of Ce addition on RIS behaviour in type 316 SS.

2. Experimental

In order to improve resistance to radiation damage of austenitic stainless steel using over-sized solute addition approach, material chosen was type 316 SS with different Ce content (0, 0.01, 0.04 and 0.09 wt%), the nominal chemical compositions of this material is given in

Table 2. The material was available in the form of 40 x 40 x 8 mm blocks with different Ce content.

Table 2: Chemical compositions of SS 316 samples with different Ce content

(Ce wt%)	C	Si	Mn	P	S	Ni	Cr	Mo
0.00	0.058	0.54	1.20	< 0.0005	0.002	13.02	16.92	2.22
0.01	0.066	0.54	1.20	< 0.0005	0.004	12.84	16.84	2.22
0.04	0.065	0.55	1.20	< 0.0005	0.002	13.11	16.91	2.24
0.09	0.064	0.57	1.15	< 0.0005	0.002	12.83	17.16	2.26

Samples of were irradiated using 4.8 MeV at 300^{o}C. Samples were cut in size of 12 x 12 x 0.5 mm and a hole of 0.5 mm was drilled on each sample to facilitate the measurement of total Columbus during experiment. The total amount of irradiation for each sample was 9.724 x 10^{17} p/cm^{2}. Irradiated samples were characterized using DL-EPR followed by AFM. DL-EPR tests for irradiated samples were carried out at room temperature (27^{o}C) in 1.0M H_2SO_4 + 0.1M KSCN solution with the scan rate of 6 V/h. It is known that the damage profile of proton irradiation is such that, the most damaged area lies at around 70 μm below the surface for 4.8 MeV protons. So that starting for as-irradiated surface, DL-EPR tests were carried out till the unaffected (not affected by irradiation) material is reached. After each test, samples were polished carefully to remove affected layer.

3. Results and Discussion

DL-EPR Test after Irradiation

The results of DL-EPR tests are given in Table 3 and graphically presented in figure 1. The DL-EPR values for sample containing Ce-0.00% shows a peak (DL-EPR value-0.114) after the removal of 70 μm depth in the 6th EPR test and after this it again decreases in 7th EPR (DL-EPR value-0.027) as shown in Table 2.

Table 3: EPR-DOS values for SS-316 irradiated samples with different Ce wt%, values in bracket show the depth from the top surface (in μm) at various stages.

Ce (wt %)	**1st EPR**	**2nd EPR**	**3rd EPR**	**4th EPR**	**5th EPR**	**6th EPR**
0.00	0.0861 (0)	0.0318 (20)	0.0224 (30)	0.0295 (40)	0.0454 (60)	0.1143 (70)
0.01	0.0851 (0)	0.7445 (30)	1.097 (60)	___		
0.04	0.3754 (0)	0.0735 (30)	0.09 (40)	0.062 (60)		
0.09	0.9154 (0)	1.007 (30)	0.715 (40)	0.0186 (70)		

For sample containing Ce 0.01 wt% and 0.01 wt%, it comes after a removal of 70 μm and 80 μm depth respectively as shown in Table 2. This shows the depth at which actual irradiation damage occurred after proton irradiation. For samples Ce 0.04 wt% and Ce 0.09 wt%, no such peak was noticed. Figure 1 shows optical micrographs of SS 316 samples after DL-EPR

of irradiated samples at a depth where maximum DL-EPR values were obtained. The micrographs of samples containing Ce-0.00% and Ce-0.01% show extensive slip lines and attack during DL-EPR was more on slip lines as compared to grain boundaries. Slip lines are strained regions within grains and act as a defect sink. The absorption of point defects (interstitial and vacancies) at slip lines required less driving forces as compared to that at the grain boundaries. Therefore, point defects preferentially get annihilated at slip lines. The sample of SS 316 Ce 0.09 wt% did not show any slip lines. Pits like features are more predominant in samples containing 0.01% and 0.09% Ce as depicted in figure 1.

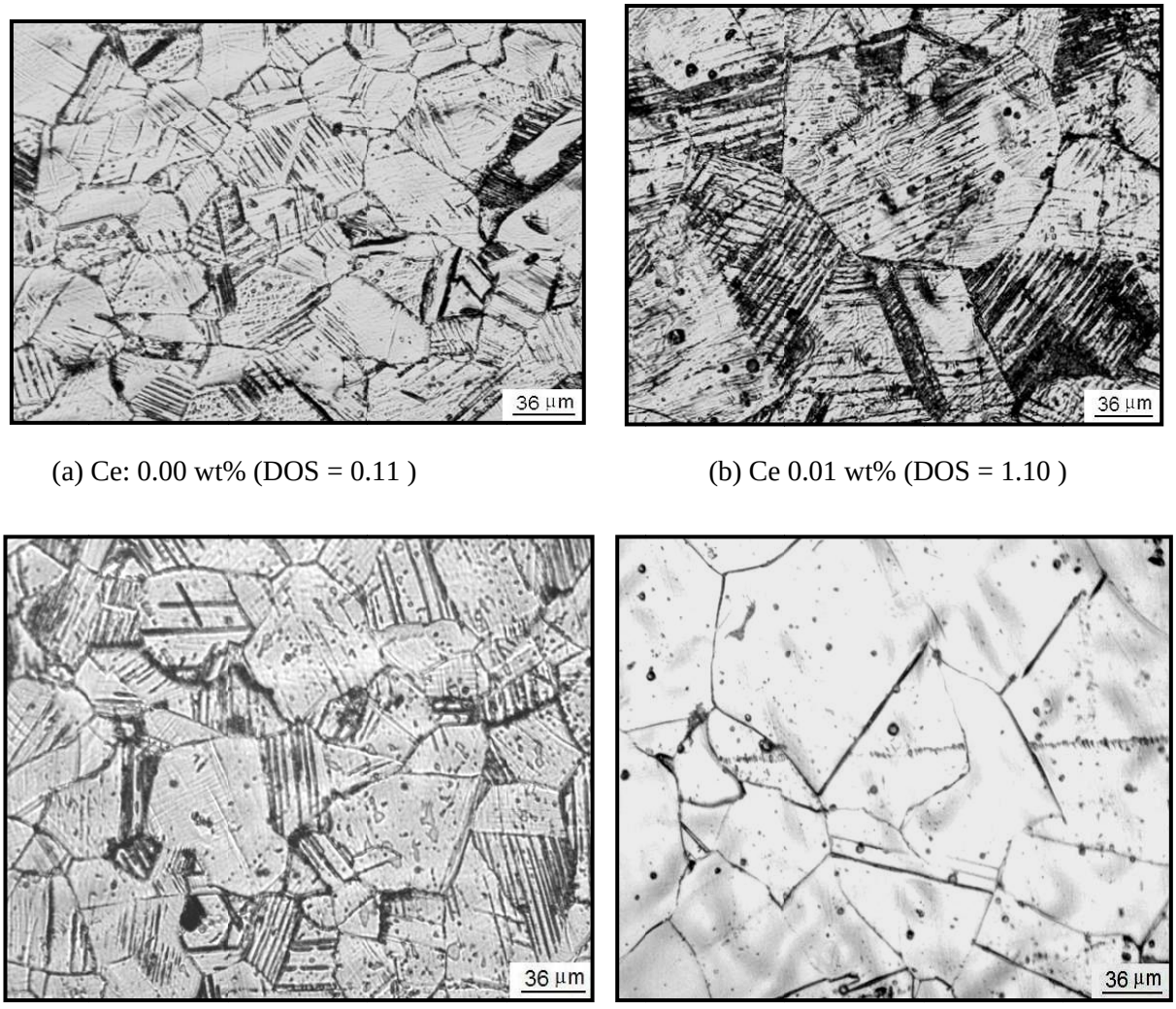

(a) Ce: 0.00 wt% (DOS = 0.11)

(b) Ce 0.01 wt% (DOS = 1.10)

(c) Ce: 0.04 wt% (DOS = 0.09)

(d) Ce 0.09 wt% (DOS = 0.72)

Figure 1: Optical micrographs of samples after proton-irradiation and DL-EPR test. As shown in figure, slip-lines were got preferentially attacked and pit-like features were predominant in 0.01 and 0.09 wt% Ce samples

AFM Examination after DL-EPR Test of Irradiated Samples

Proton irradiated samples were examined using AFM after DL-EPR tests to determine the extent of RIS -in terms of the depth of attack at grain boundaries and slip lines. Samples were examined in semi-contact mode after each EPR test. Table 4 depicts the extent of attack (depth) in SS 316 Ce samples after DL-EPR tests. It shows typical values of depths evaluated at various points in the microstructure after AFM examinations.

It can be seen from the Table 4, SS 316 Ce 0.00 wt% sample did not show any pit-like features while all Ce containing samples showed pit-like features. Sample with 0.09 wt% Ce did not have any slip lines hence, most of attack has occurred on grain boundaries. The maximum depth of pit-like features in sample 0.01wt% Ce was 1.2 µm. Figure 2 shows an AFM micrograph of SS 316 Ce 0.00 wt% sample after DL-EPR test.

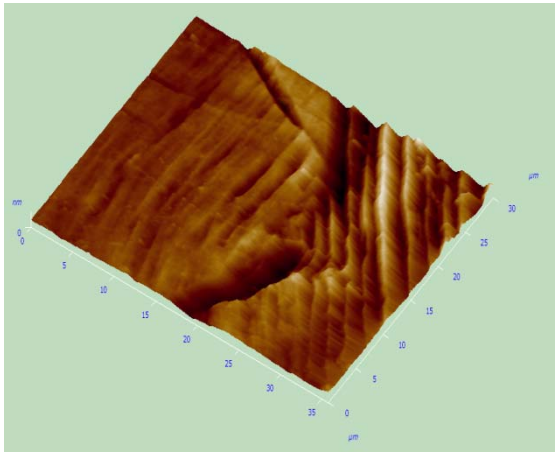

(a) Ce: 0.00 wt% (DOS = 0.11)

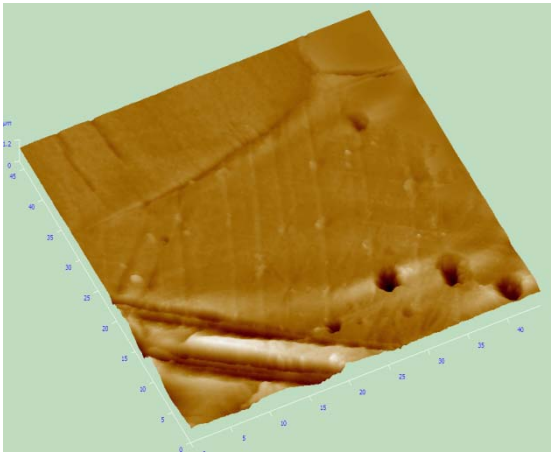

(b) Ce 0.01 wt% (DOS = 1.10)

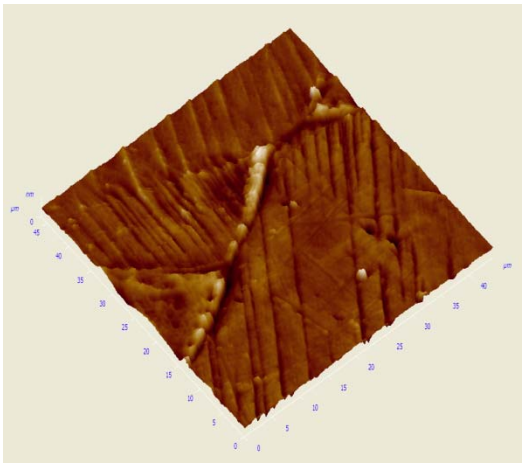

(c) Ce: 0.04 wt% (DOS = 0.09)

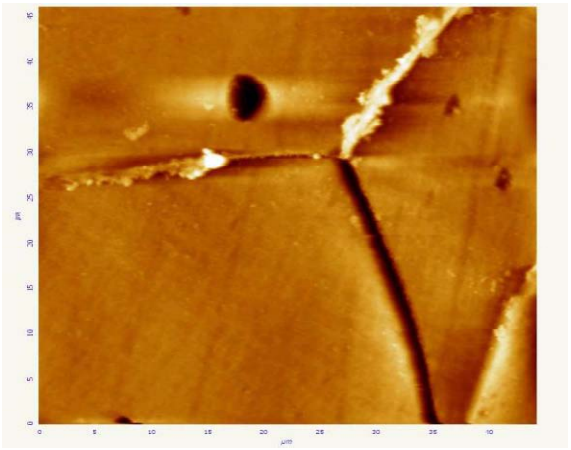

(d) Ce 0.09 wt% (DOS = 0.72)

Figure 2: AFM micrographs of samples after proton-irradiation and DL-EPR test. As shown in figure, slip-lines were got preferentially attacked and pit-like features were predominant in 0.01 and 0.09 wt% Ce samples. Grain boundary attack was clearly noticed in 0.09 wt% Ce sample.

Table 4: Depths of attack on SS 316 Ce samples after DL-EPR tests as measured by AFM examination

Ce (wt%)	Slip lines (nm)	Grain Boundaries (nm)	Pits (nm)
0.00	90 – 500	80 – 600	-
0.01	200 – 500	40 - 100	400 – 1200
0.04	120 – 500	80 – 600	250 – 400
0.09	-	80 – 400	100 - 500

AFM micrographs show the nature of attack on various microstructural features after DL-EPR tests of irradiated SS 316 Ce samples. It can be seen from the figure that for 0.00, 0.01 and 0.04 wt%Ce samples, attack was predominantly on slip lines indicating slip lines were preferred defect sink with respect to grain boundaries.

4. Conclusion

- It was shown in this study that the extent of RIS (specifically Cr depletion) can be characterized using DL-EPR technique
- AFM technique was used to determine the extent of attack (after DL-EPR) on various microstructural features like slip lines and grain boundaries
- Sample with Ce-0.04% showed better resistance towards RIS, as measured by DL-EPR
- High resistance towards RIS for Ce added samples is due to more depletion of chromium within the grain along slip lines around Ce atom as compared to grain boundaries
- Pit-like features are more predominant in 0.01% Ce and 0.09% Ce samples

References:

1. H. Watanbe, T. Muroga, N. Yshida, *J Nucl Mater*, **239**(1996)95
2. N. Shigenaka, S. Ono, Y. Isobe, T. Hashimoto, H. Fujimori, S. Uchida, *J Nucl Sci Tech,* **33**(7)(1996)577
3. S. Kasahara, K. Nakata, K. Fukuya, S. Shima, A.J Jacobs, G.P. Wozadlo, S. Suzuki, in: *"Proc of the Sixth International Symposium on Environmental Degradation of Materials in Nuclear Power, Systems Water Reactors*", 15 August, San Diego, CA, The Minerals, Metals and Materials Society (1993)615
4. N. Sakaguchi, S. Watanabe, H. Takahashi, Nucl Instrum and Meth B, **153**(1999) 142
5. T. Kato, H. Takahashi, M. Izumiya, *J Nucl Mater*, **189**(1992)167
6. M.A. Ashworth, D.I.R. Norris, I.P. Jones, *J Nucl Mater*, **189**(1992)289
7. S. Ohnuki, S. Yamashita, H. Takahashi, T. Kato, in: "*Proc of the 19th International Symposium on the Effects of Radiation on Materials"*, 16-18 June, Seattle, WA, American Society for Testing and Materials, (1999)756
8. S. Dumbill, W. Hanks, in: "*Proc of the Sixth International Symposium on Environmental Degradation of Materials in Nuclear Power Systems Water Reactors"*, 15 August, San Diego, CA, The Minerals, Metals and Materials Society (1993) 521
9. L. Fournier,B.H. Sencer, G.S. Was, E.P. Simonen, S.M. Bruemmer, *J Nucl Mater*, **321**(2003)192-209
10. P.J. Maziasz, C.J. McHargue, *Int Met Rev* **32** (1987)
11. Y. C. Lu and M. B. Ives, *Corros Sci* **39** (1993)1773
12. Y. C. Lu and M. B. Ives, *Corros Sci* **37**(1995)145
13. Y. Nakamura, *Metall Trans* **5**(1974)909
14. Y. Saito, T. Kiryu, T. Kimura, T. Amano, and K. J. Yajima*, Jpn inst Metals* **39**(1975)1110
15. Y. Watanabe, V. Kain, T. Tonozuka, T. Shoji, T. Kondo and F. Masuyama, *Scripta Mater* **42**(2000)307-312
16. Y. Watanabe, T. Tonozuka, T. Shoji, T. Kondo, *Corrosion* **99**, Paper No. 453(1999)1-10